Organic & Biomolecular Chemistry

PAPER

View Article Online
View Journal | View Issue

Cite this: *Org. Biomol. Chem.*, 2014, **12**, 2792

Evaluating *N*-benzylgalactonoamidines as putative transition state analogs for β-galactoside hydrolysis†

Qiu-Hua Fan, Susanne Striegler,* Rebekah G. Langston and James D. Barnett

Received 21st January 2014,
Accepted 7th March 2014

DOI: 10.1039/c4ob00153b

www.rsc.org/obc

Experimental evidence is provided for *p*-methylbenzyl-D-galactonoamidine to function as a true transition state analog for the enzymatic hydrolysis of aryl-β-D-galactopyranosides by β-galactosidase (*A. oryzae*). The compound exhibits inhibition constants in the low nanomolar concentration range (12–56 nM) for a selection of substrates. Along these lines, a streamlined synthetic method based on phase-transfer catalysis was optimized to afford the required variety of new aryl-β-D-galactopyranosides. Last, the stability of the galactonoamidines under the assay conditions was confirmed.

Introduction

Emerging evidence suggests that the glycosidase family includes multiple mechanistic pathways for glycoside hydrolyses.[1] Given this observation, the prediction of whether or not a given compound is a true transition state analog (TSA) for the cleavage of a glycosidic bond by the glycosidase of interest remains speculative and must be confirmed by experimental evaluation. Such investigation becomes particularly valuable when a putative TSA is not only to be identified as a very potent enzymatic inhibitor, but to be used subsequently for the preparation of catalytic material such as functional enzyme mimics. As a prerequisite, a potential TSA must behave as a competitive inhibitor, and not as a non-competitive or mixed inhibitor, to ensure interaction inside the active site rather than fortuitous binding outside the active site of an enzyme.[2]

To experimentally categorize a compound as a TSA, kinetic experiments with either mutants of the targeted enzyme or various structurally related derivatives of the original substrate are sufficient.[2] The correlation of the inhibition constant (K_i) *versus* the catalytic efficiency (k_{cat}/K_m) for a variety of substrates should reveal a value close to 1 for a linear correlation on a logarithmic scale if the compound is a true transition state analog of the reaction; the value of the linear correlation will be very different from 1, if not.[2–5]

We previously examined the inhibitory effects of aryl-D-galactonoamidines (**1a–e, g**) (Chart 1) on the enzymatic hydrolysis of commercially available 2-nitrophenyl-β-D-galactopyranoside (**2a**) as a model reaction.[6]

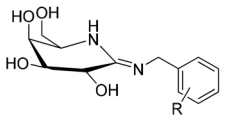

1a: R = H
1b: R = o-Me
1c: R = m-Me
1d: R = p-Me
1e: R = o-F
1f: R = m-F
1g: R = p-F

Chart 1 Structures of aryl-D-galactonoamidines (**1a–g**).

The previous studies disclosed **1a–e** and **1g** as competitive inhibitors with inhibition constants (K_i) in the low nanomolar concentration range (12–48 nM).[6] Not all of these compounds may fulfill the experimental requirements for a TSA, but they may resemble fortuitous binders in the active site of β-galactosidase (*A. oryzae*) instead. Prior to the preparation of catalytic microgels from such aryl-D-galactonoamidines, it is thus imperative to experimentally select a compound with true transition state-like character for the hydrolysis of glycosidic bonds.

Along these lines, we report here our preliminary results to identify *N*-arylgalactonoamidine **1d** as a putative transition state analog for the enzymatic hydrolysis of β-D-galactopyranosides. We additionally provide analytical data for **1f** and evidence for the stability of the *N*-arylgalactonoamidines under the experimental conditions. We furthermore report the synthesis and full characterization of 12 new aryl-β-D-galactopyranosides (**2b–g** and **2i–n**) as substrates for the spectroscopic evaluation of β-galactosidases.

Results and discussion

In order to determine the transition state-like character of the galactonoamidines **1a–f**, β-galactosidase (*A. oryzae*) was used

119 Department of Chemistry and Biochemistry, University of Arkansas, Fayetteville, AR 72701, USA. E-mail: susanne.striegler@uark.edu

† Electronic supplementary information (ESI) available: ^{1}H and ^{13}C NMR spectra of all new aryl-tetra-*O*-acetyl-β-D-galactopyranosides **4b–g**, **4i–r**, aryl-β-D-galactopyranosides **2b–g**, **2i–r** and galactonoamidine **1f**. See DOI: 10.1039/c4ob00153b

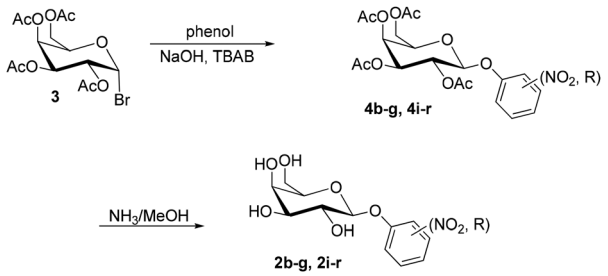

Scheme 1 Synthesis of aryl-β-D-galactopyranosides substrates **2b–g** and **2i–r**.

as model catalyst.[6,7] Unfortunately, the spectroscopic evaluation of β-galactosidases with commercial substrates is limited to 2-nitro- and 4-nitrophenyl-β-D-galactopyranoside **2a** and **2h**, respectively. In need of structurally related aryl-β-D-galactopyranosides, we initially synthesized and characterized 15 new aryl-β-D-galactopyranosides **2b–g** and **2i–r** (Scheme 1) taking advantage of synthetic procedures toward related compounds described previously by Thiem *et al.*[8]

Along these lines, we reacted a selection of commercially available phenols with peracetylated α-galactosyl bromide (**3**) using a tetrabutylammonium bromide-catalyzed glycosylation in alkaline solution (Scheme 1, Table 1).[8] Chromatographic purification of the obtained tetraacetylaryl-β-D-galactopyranosides **4b–g, i–r** over silica gel and subsequent deacetylation with ammonia in methanol afforded the target glycosides **2b–g, i–r** in moderate to good yields (60–85%).

Table 1 Arylglycosides **2a–n** and the molar absorptivity of their aryl aglycon in 50 mM acetate buffer at pH 5 and 30 °C

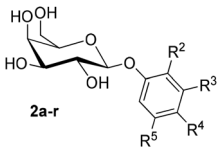

Entry	S	R^2	R^3	R^4	R^5	ε_{405} [b]
1	**2a**[a]	NO_2	H	H	H	450
2	**2b**	NO_2	H	Me	H	1083
3	**2c**	NO_2	H	F	H	851
4	**2d**	NO_2	H	Cl	H	936
5	**2e**	NO_2	H	Br	H	1047
6	**2f**[c]	NO_2	H	H	F	495
7	**2g**	NO_2	H	H	Me	538
8	**2h**[a]	H	H	NO_2	H	223
9	**2i**[c]	F	H	NO_2	H	3145
10	**2k**[c]	Cl	H	NO_2	H	5595
11	**2l**	H	NO_2	Me	H	152
12	**2m**	H	NO_2	Cl	H	104
13	**2n**	H	NO_2	H	H	56
14	**2o**	NO_2	Me	H	H	182
15	**2p**	NO_2	H	MeO	H	2678
16	**2q**	Me	H	NO_2	H	288
17	**2r**	H	Me	NO_2	H	209

[a] Commercially available. [b] ε [M^{-1} cm^{-1}] is the molar extinction coefficient of the phenolate in 50 mM acetate buffer at pH 5 and 30 °C. [c] Known.[8,11]

With a variety of substrates available, we then developed kinetic assays in 96-well plate format to monitor the product formation of the enzymatic glycoside hydrolysis in the presence or absence of galactonoamidines **1a–g** using UV/Vis spectroscopy at 405 nm. The protein concentration of the commercially available β-galactosidase (*A. oryzae*) was previously determined by a BCA assay.[6] Conversion of the measured absorbance into product concentration was achieved with calibration curves for the molar absorptivity for each substrate under the given experimental conditions. The high absorption coefficient of 2-chloro- and 2-fluoro-4-nitrophenyl-β-D-galactopyranoside renders these two substrates superior to commercially available **2a** and **2h**, especially for assays requiring acidic conditions. Compounds **2l–o**, **2q,r** were not used for evaluating the enzymatic hydrolysis by UV/Vis spectroscopy due to the low absorptivity of the resulting phenolates under the reaction conditions and the accompanying uncertainty of the data. Galactopyranoside **2p** was found to show surprising low water solubility under the used condition limiting its usage in this assay as well.

The rate of the reaction was corrected for the enzyme concentration and the uncatalyzed reaction, and then plotted *versus* the substrate concentration. By applying a non-linear fit to the resulting hyperbolic data, the catalytic rate constant k_{cat} [min^{-1}] and the substrate affinity K_M [mM] were discerned utilizing the Michaelis–Menten model (Table 2). In the presence of galactonoamidines, apparent Michaelis–Menten constants (K'_m) and rate constants (k'_{cat}) were determined in a similar fashion and allowed the calculation of the inhibition constant (K_i) for each substrate (Table 2).

All compounds **1a–g** are very potent inhibitors that hamper the enzymatic hydrolysis of the selected substrates **2a–k** in the low nanomolar concentration range (8–63 nM). To evaluate their potency as putative transition state analogs, we correlated the catalytic efficiency of the uninhibited enzymatic catalysis for each substrate (**2a–k**) to the corresponding inhibition constant of galactonoamidines **1a–g.** A reasonable correlation with a value close to 1 is observed for **1d**, while the correlations obtained for **1b**, **1c** (Fig. 1) and for **1e** and **1g** (Fig. 2) clearly result in scattered data, a linear factor (a) very different from 1, and an overall very poor correlation factor (R^2) for the fit of the data. A reasonable correlation with a value close to 1 is also observed for **1f** (Fig. 2) and **1a** (data not shown), but the correlation factors for the fit of the data are not as good as for **1d.** Consequently, we propose **1d**, *p*-methylbenzyl-D-galactonoamidine, as a true transition state analog for the enzymatic hydrolysis of β-D-galactopyranosides by β-galactosidase (*A. oryzae*).

Subsequently, the stability of **1d** under various pH conditions was studied prior to further investigation of the inhibition of other glycosidases or the preparation of biomimetic catalysts derived therefrom. Galactonoamidine **1d** was found stable for a minimum of 3 h, when exposed to nanopure water at 30, 50 or 72 °C. Likewise, no evidence for compound decomposition was observed by HPLC assays relying on a carbohydrate-discriminating Na^+-RMN column as stationary phase and nanopure water as eluent, when exposing **1d** to

Table 2 Kinetic parameters for the evaluation of **1a–g** as putative transition state analogs

Entry	S	k_{cat} [min^{-1}]	K_M [mM]	K_i [**1a**] × 10^{-9} [M]	K_i [**1b**] × 10^{-9} [M]	K_i [**1c**] × 10^{-9} [M]	K_i [**1d**] × 10^{-9} [M]	K_i [**1e**] × 10^{-9} [M]	K_i [**1f**] × 10^{-9} [M]	K_i [**1g**] × 10^{-9} [M]
1	**2a**	4590	1.27	20.8	14.8	24.6	23.3	17.3	16.4	18.6
2	**2b**	4808	1.49	22.9	9.7	22.7	14.1	22.9	22.3	11.1
3	**2c**	4658	1.24	18.4	9.7	20.6	13.3	12.0	18.1	11.0
4	**2d**	4138	0.96	14.6	7.6	22.8	11.6	8.7	13.3	8.7
5	**2e**	3882	1.10	15.9	10.3	22.6	16.5	24.6	14.2	11.4
6	**2f**	3886	1.78	25.7	17.1	28.8	24.6	11.1	30.3	62.7
7	**2g**	4209	4.27	37.1	22.8	45.2	55.7	28.0	58.1	31.0
8	**2h**	3238	0.84	16.1	17.0	26.7	15.1	20.9	22.8	14.6
9	**2i**	3670	0.92	14.8	22.2	26.2	11.5	12.2	13.7	15.0
10	**2k**	2381	0.70	21.1	23.6	29.4	8.0	16.1	20.3	10.1

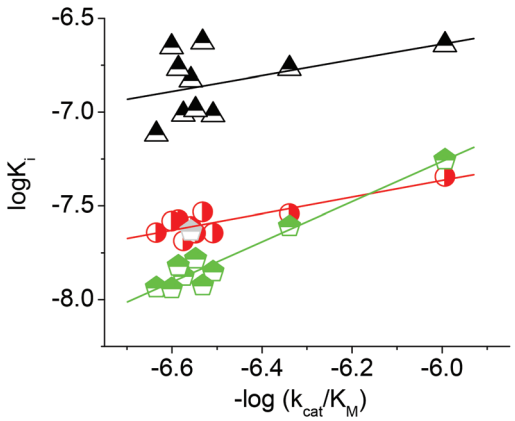

Fig. 1 Double-logarithmic correlation between the catalytic efficiency (k_{cat}/K_M) and the inhibition constant (K_i) with linear fit $y = ax + b$ for 11 nitrophenyl-β-D-glycosides in the presence of **1b** (black triangle), a = 0.42, R^2 = 0.201; **1c** (red circle), a = 0.44; R^2 = 0.766; **1d** (green pentagon); a = 1.07; R^2 = 0.946.

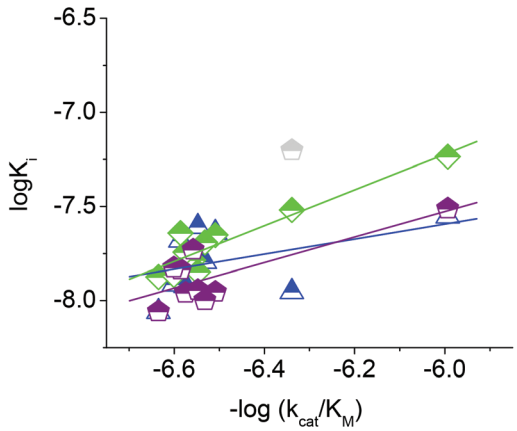

Fig. 2 Double-logarithmic correlation between the catalytic efficiency (k_{cat}/K_M) and the inhibition constant (K_i) with linear fit $y = ax + b$ for 11 nitrophenyl-β-D-glycosides in the presence of **1e** (blue triangle), a = 0.40, R^2 = 0.204; **1f** (green diamond), a = 0.95; R^2 = 0.869; 1 g (purple pentagon); a = 0.67; R^2 = 0.625.

acetate buffer at 30 °C for the same amount of time. However, the glyconoamidine stability under alkaline conditions is debated in the literature,[9–14] and insufficient stability of **1d** in conditions previously used for the preparation of microgels, *i.e.* 50 mM CAPS buffer at pH 10.5 and 72 °C, was noted. Recent preliminary results disclose sufficient stability of **1d** in 5 mM CAPS buffer at pH 10.5 and 0 °C or 5 mM TAPS buffer at pH 9 and 10 °C. As the preparation of enzyme mimics at elevated pH is envisioned, related studies are ongoing.

Conclusions

The preparation of functional enzyme mimics based on a template resembling a transition state analog-like structure ideally includes an experimental evaluation of the compound prior to its use to critically evaluate its potential. Along these lines, a kinetic approach was used that relies on the correlation of the inhibition constants (K_i) of the target compound to the catalytic efficiency (k_{cat}/K_M) in the presence of various structurally related substrates. Overall, 7 galactonoamidines, all previously identified as competitive inhibitors, were evaluated and *p*-methylbenzyl-D-galactonoamidine **1d** (K_i = 8–56 nM) was identified here as a putative TSA for the hydrolysis of β-galactopyranosides by β-galactosidase (*A. oryzae*). The results obtained indicate a strong stereoelectronic effect of the *p*-substituted position of the aromatic aglycon in the selected aryl-D-galactonoamidines that influences both the binding affinity of the inhibitors **1a–g** and their ability to function as transition state analogs during the enzymatic hydrolysis of β-D-galactopyranosides. The presented results provide the foundation for the evaluation of galactonoamidine **1d** as an inhibitor and a putative TSA of other glycosidases, and their transition state-like features, and its use as TSA during preparation of macromolecular enzyme mimics targeting the hydrolysis and synthesis of glycosidic bonds.

Experimental

Instrumentation

^{1}H and ^{13}C NMR spectra were recorded on a 400 MHz Bruker magnet with *Z* gradient and 5 mm broadband head using

Topspin 2.1 software. IR spectra were obtained on a Perkin-Elmer Spectrum 100 FT-IR spectrophotometer with Perkin-Elmer spectrum express software versions 1.01.00. High resolution mass spectrometry data were obtained in the state-wide mass spectrometry facility at Arkansas University on a Bruker ultrOTOF-Q quadrupole time-of-flight (qQ-TOF) mass spectrometer equipped with an electrospray ionization source or the Mass Spectrometry Facility at Georgia State University, Atlanta, GA. Combustion data were obtained from Atlantic Microlab, Atlanta, GA. UV/Vis data were recorded on a FilterMax F5 Multi-Mode Microplate Reader from Molecular Devices using 96 well, medium-binding microlon Elisa-plates from Greiner Bio-one. Lyophilization was performed on a FreeZone 1 liter benchtop freeze dry system from Labconco. Melting points were recorded on a Mel-Temp melting point apparatus, and the values are uncorrected. Nanopure water at a resistance of 18.2 mΩ was obtained from a ThermoScientific Barnstead E-pure™ water purification system. The stability assays were performed on an HPLC system from Shimadzu equipped with SCL-10Avp system controller, 2 LC-20AD analytical pumps, DGU-20A3R three channel online degassers, SIL-20A UFLC autosampler with 96 well capability, CTO-20A/prominence column oven and ELSD-90LT light scattering and LC solution software, version 1.25 from Shimadzu for data recording and analysis.

Materials and methods

Chemical shifts (δ) in NMR data are expressed in parts per million (ppm) and coupling constants (J) in Hz. Signal multiplicities are denoted as s (singlet), d (doublet), t (triplet), q (quartet) and m (multiplet). Deuterated chloroform, acetone-d6, DMSO-d_6 and deuterium oxide were used as solvents. Chemical shift values are reported relative to the residual signals of these solvents ($CDCl_3$, δ_H 7.29, δ_C 77.0; acetone-d_6, δ_H 2.05, δ_C 29.8; DMSO-d_6, δ_H 2.50, δ_C 39.5; D_2O: δ_H 4.80 δ_C 29.8 after addition of a few drops of acetone-d_6. High resolution mass spectrometry data were obtained from samples that were mixed with acetonitrile containing 0.1% formic acid and injected into the source *via* syringe pump operating at 3 μL h^{-1}. The dry gas temperature was 180 °C, the dry gas flow was 5 L min^{-1}, and the nebulizing gas pressure was 1 bar. The remaining instrument parameters were optimized to obtain maximum signal for ions between 100–1000 amu. IR data were obtained as thin films on KBr discs or as KBr pellets (ν in cm^{-1}) with a resolution of 0.5 cm^{-1}.

Column chromatography was carried out using silica gel 60 from Silicycle® (40–63 μm, 230–240 mesh). Thin layer chromatography (TLC) was performed using silica gel TLC plates from SORBENT Technologies, 200 μm, 4 × 8 cm, aluminum backed, with fluorescence indicator F_{254} and detection by UV light or by charring with an ethanolic vanillin-sulfuric acid reagent and subsequent heating of the TLC plate.

All pH values were obtained using a Beckman Φ 250 pH meter equipped with a refillable ROSS combination pH electrode from Orion with epoxy body and a 8 mm semi-micro tip. The pH meter was calibrated before each set of readings (3-point calibration).

All commercially obtained chemicals had reagent grade quality or better and were used as received, if not noted otherwise. Per-acetylated galactosyl bromide was prepared as described.[15,16] All phenols 2-nitrophenol, 3-nitrophenol, 4-nitrophenol, 4-fluoro-2-nitrophenol, 4-chloro-2-nitrophenol, 4-bromo-2-nitrophenol, 3-methyl-2-nitrophenol, 4-methoxy-2-nitrophenol, 4-methyl-2-nitrophenol, 5-fluoro-2-nitrophenol, 5-methyl-2-nitrophenol, 4-methyl-3-nitrophenol, 4-chloro-3-nitrophenol, 2-methyl-4-nitrophenol, 3-methyl-4-nitrophenol, 2-chloro-4-nitrophenol, 2-fluoro-4-nitrophenol and 3-iodo-4-nitrophenol were sublimed, recrystallized from water or purified by column chromatography on silica gel using ethyl acetate and hexane as eluent prior to the determination of their extinction coefficients.

β-Galactosidase [3.2.1.23] from *Aspergillus oryzae* was obtained from Sigma-Aldrich as lyophilized powder stabilized on dextrin and stored at −18 °C. A BCA assay confirmed that the supplied batch contains 10% of protein.[6] The molar weight of the tetrameric protein was determined as 347.2 kDa (86.8 kDa per unit) by microchip electrophoresis.[6]

Synthetic procedures

Synthesis of inhibitors: general procedure yielding *N*-benzyl-D-galactonoamidines. The galactonoamidines **1a–g** were prepared as described previously.[6,7] Sufficient analytical data for **1f** were obtained after repetitive purification of the precursor compound as described previously, and are summarized below.

3-Fluorobenzyl-D-galactonoamidine (1f). *m*-Fluorobenzyl-2,3,4,6-tetra-*O*-benzyl-β-D-galactonoamidine[6] (64.0 mg, 0.1 mmol) and 128.0 mg 10% Pd on charcoal (0.06 mmol, 0.6 eq.) were stirred under hydrogen in 7.5 mL ethanol in the presence of 1.5 mL (19.5 mmol) trifluoroacetic acid at ambient temperature for 24 h. The mixture was filtered through a pad of celite, and the celite was washed three times with 2 mL methanol. The combined filtrates were concentrated under reduced pressure, and the resulting residue was lyophilized yielding **1f** as a very hygroscopic, colourless foam in 95% yield (27.0 mg, 0.095 mmol); R_f 0.25 (SiO_2, MeOH); δ_H (D_2O) 7.38 (dd, 14.8, 7.5, 1H), 7.00–7.16 (m, 3H), 4.55–4.68 (m, 3H), 4.26 (br. s., 1H), 3.95 (dd, 10.0, 2.0, 1H), 3.70–3.78 (m, 2H), 3.66 (dd, 13.3, 9.8, 1H); δ_C (D_2O + MeOH-d_4) 165.5, 163.9 ($^1J_{C,F}$ = 245.0 Hz), 137.3 ($^3J_{C,F}$ = 7.3 Hz), 131.8 ($^3J_{C,F}$ = 8.1 Hz), 124.0 ($^4J_{C,F}$ = 2.9 Hz), 116.2 ($^2J_{C,F}$ = 21.3 Hz), 115.0 ($^2J_{C,F}$ = 22.7 Hz), 71.6, 68.0, 67.5, 60.9, 58.4, 45.6 ($^4J_{C,F}$ = 2.0 Hz; HR-ESI MS found: 285.1248, calculated for $C_{13}H_{18}FN_2O_4$, $[M + H]^+$: 285.1251.

Synthesis of substrates: general procedure yielding aryl-tetra-*O*-acetyl-β-D-galactopyranosides.[8] The syntheses of the title compounds were achieved by phase-transfer-catalyzed glycosylation of phenols with peracetylated galactosyl bromide.[15,16] Chromatographic purification of the raw material on silica gel yielded the title compounds in moderate to good yields. The

eluent consisted of cyclohexane–ethyl acetate mixtures if not noted otherwise.

4-Methyl-2-nitrophenyl-tetra-*O*-acetyl-β-D-galactopyranoside (4b). Off-white solid; mp 188–190 °C; R_f 0.25 (SiO_2, cyclohexane–ethyl acetate = 3/2, v/v); δ_H ($CDCl_3$) 7.58 (d, 1.5, 1 H), 7.40–7.17 (m, 2 H), 5.52 (dd, 10.5, 8.0, 1 H), 5.48–5.40 (m, 1 H), 5.09 (dd, 10.5, 3.4, 1 H), 5.02 (d, 8.1, 1 H), 4.25 (dd, 11.2, 6.9, 1 H), 4.16 (dd, 11.6, 6.3, 1 H), 4.09–3.95 (m, 1 H), 2.18 (s, 3 H), 2.13 (s, 3 H), 2.06 (s, 3 H), 2.01 (s, 3 H); δ_C ($CDCl_3$) 170.3, 170.2, 170.1, 169.4, 147.0, 141.2, 134.2, 134.1, 125.1, 120.1, 101.0, 71.2, 70.5, 67.8, 66.7, 61.3, 20.6, 20.6, 20.5, 20.4; Calcd for $C_{21}H_{25}NO_{12}$ C, 52.17; H, 5.21; N, 2.90; found: C, 52.08; H, 5.21; N, 2.92.

4-Fluoro-2-nitrophenyl-tetra-*O*-acetyl-β-D-galactopyranoside (4c). Off-white solid; mp 172–173 °C; R_f 0.28 (SiO_2, cyclohexane–ethyl acetate = 3/2, v/v); δ_H ($CDCl_3$) 7.53 (dd, 7.6, 3.0, 1 H), 7.41 (dd, 9.3 Hz, 4.5), 7.30–7.20 (m, 1 H), 5.51 (dd, 10.5, 8.0, 1 H), 5.45 (dd, 3.4, 0.9, 1 H), 5.09 (dd, 10.5, 3.4, 1 H), 5.01 (d, 7.8, 1 H), 4.25 (dd, 11.2, 6.9, 1 H), 4.15 (dd, 11.4, 6.3, 1 H), 4.08–4.00 (m, 1 H), 2.21–2.16 (m, 3 H), 2.12 (s, 3 H), 2.05 (s, 3 H), 2.00 (s, 3 H); δ_C ($CDCl_3$) 170.2, 170.1, 170.0, 169.4, 157.5 ($^1J_{C,F}$ = 248.8 Hz), 145.4 ($^4J_{C,F}$ = 2.9 Hz), 122.5 ($^3J_{C,F}$ = 8.1 Hz), 120.5 ($^2J_{C,F}$ = 22.7 Hz), 112.3 ($^2J_{C,F}$ = 27.8 Hz), 101.2, 71.4, 70.4, 67.8, 66.6, 61.2, 20.6, 20.6, 20.6, 20.5; Calcd for $C_{20}H_{22}FNO_{12}$ C, 49.29; H, 4.55; N, 2.87. Found: C, 49.13; H, 4.65; N, 2.87.

4-Chloro-2-nitrophenyl-tetra-*O*-acetyl-β-D-galactopyranoside (4d). Off-white solid; mp 192–193 °C; R_f 0.31 (SiO_2, cyclohexane–ethyl acetate = 3/2, v/v); δ_H ($CDCl_3$) 7.79 (d, 2.5, 1 H), 7.49 (dd, 8.8, 2.5, 1 H), 7.34 (d, 8.8, 1 H), 5.53 (dd, 10.5, 8.0, 1 H), 5.47 (d, 3.0, 1 H), 5.10 (dd, 10.6, 3.3, 1 H), 5.05 (d, 7.8, 1 H), 4.25 (dd, 11.4, 7.1, 1 H), 4.16 (dd, 11.4, 6.1, 1 H), 4.10–4.02 (m, 1 H), 2.19 (s, 3 H), 2.13 (s, 3 H), 2.07 (s, 3 H), 2.02 (s, 3 H); δ_C ($CDCl_3$) 170.2, 170.1, 170.1, 169.4, 147.8, 141.6, 133.5, 129.1, 125.1, 121.4, 100.8, 71.5, 70.4, 67.7, 66.6, 61.3, 20.6, 20.6, 20.5; Calcd for $C_{20}H_{22}ClNO_{12}$ C, 47.68; H, 4.40; N, 2.78. Found: C, 47.65; H, 4.42; N, 2.74.

4-Bromo-2-nitrophenyl-tetra-*O*-acetyl-β-D-galactopyranoside (4e). Off-white solid; mp 198–199 °C; R_f 0.30 (SiO_2, cyclohexane–ethyl acetate = 3/2, v/v); δ_H ($CDCl_3$) 7.92 (d, 2.3, 1 H), 7.62 (dd, 8.8, 2.5, 1 H), 7.25 (d, 1.5, 1 H), 5.52 (dd, 10.4, 8.1, 1 H), 5.45 (d, 2.5, 1 H), 5.08 (dd, 10.5, 3.4, 1 H), 5.03 (d, 8.1, 1 H), 4.23 (dd, 11.4, 7.1, 1 H), 4.15 (dd, 11.4, 6.1, 1 H), 4.09–4.00 (m, 1 H), 2.18 (s, 3 H), 2.11 (s, 3 H), 2.06 (s, 3 H), 2.00 (s, 3 H); δ_C ($CDCl_3$) 170.3, 170.1, 170.1, 169.3, 148.3, 141.9, 136.5, 127.9, 121.6, 115.9, 100.8, 71.5, 70.4, 67.7, 66.6, 61.3, 20.6, 20.6, 20.5; Calcd for $C_{20}H_{22}BrNO_{12}$ C, 43.81; H, 4.04; N, 2.25. Found: C, 43.67; H, 4.14; N, 2.53.

5-Fluoro-2-nitrophenyl-tetra-*O*-acetyl-β-D-galactopyranoside.[8] (4f). Off-white solid; mp 158–159 °C (lit.[8] 159 °C), R_f 0.37 (SiO_2, cyclohexane–ethyl acetate = 3/2, v/v); δ_H ($CDCl_3$) 7.90 (dd, 9.1, 5.8, 1 H), 7.14 (dd, 10.0, 2.7, 1 H), 6.96–6.82 (m, 1 H), 5.57 (dd, 10.5, 8.0, 1 H), 5.47 (dd, 3.4, 0.9, 1 H), 5.18–4.97 (m, 2 H), 4.37–3.98 (m, 3 H), 2.18 (s, 3 H), 2.14–2.11 (m, 3 H), 2.09 (s, 3 H), 2.01 (s, 3 H); δ_C ($CDCl_3$) 170.2, 170.0, 169.9, 169.2, 164.8 ($^1J_{C,F}$ = 256.9 Hz), 151.3 ($^3J_{C,F}$ = 11.7 Hz), 137.3 ($^4J_{C,F}$ = 2.9 Hz), 127.4 ($^3J_{C,F}$ = 11.0 Hz), 110.4 ($^2J_{C,F}$ = 23.4 Hz), 107.0 ($^2J_{C,F}$ = 27.1 Hz), 100.4, 70.3, 67.5, 66.7, 61.6, 20.5, 20.5, 20.4, 20.3 Calcd for $C_{20}H_{22}FNO_{12}$ C, 49.29; H, 4.55; N, 2.87. Found: C, 49.28; H, 4.63; N, 2.85.

5-Methyl-2-nitrophenyl-tetra-*O*-acetyl-β-D-galactopyranoside (4g). Off-white solid; mp 218–219 °C; R_f 0.25 (SiO_2, cyclohexane–ethyl acetate = 3/2, v/v); δ_H ($CDCl_3$) 7.72 (d, 8.3, 1 H), 7.15 (d, 1.0, 1 H), 7.03–6.91 (m, 1 H), 5.54 (dd, 10.6, 7.8, 1 H), 5.46 (dd, 3.3, 1.0, 1 H), 5.13–5.04 (m, 1 H), 4.27–4.13 (m, 1 H), 4.13–4.05 (m, 1 H), 2.18 (s, 3 H), 2.11 (s, 3 H), 2.07 (s, 3 H), 2.00 (s, 3 H); δ_C ($CDCl_3$) 170.2, 170.1, 170.1, 169.3, 149.4, 145.3, 138.9, 125.2, 124.2, 120.0, 100.6, 71.4, 70.5, 67.8, 66.8, 61.6, 21.8, 20.6, 20.6, 20.5; Calcd for $C_{21}H_{25}NO_{12}$ C, 52.17; H, 5.21; N, 2.90. Found: C, 51.89; H, 5.03; N, 2.92.

2-Fluoro-4-nitrophenyl-tetra-*O*-acetyl-β-D-galactopyranoside.[8] (4i). Off-white solid; mp 130–131 °C (lit.[8] mp 134 °C); R_f 0.31 (SiO_2, cyclohexane–ethyl acetate = 3/2, v/v); δ_H ($CDCl_3$) 8.09–8.08 (m, 1 H), 7.37–7.19 (m, 1 H), 5.54 (dd, 10.5, 8.0, 1 H), 5.47 (dd, 3.4, 0.9, 1 H), 5.20–5.04 (m, 2 H), 4.29–4.02 (m, 3 H), 2.19 (s, 3 H), 2.12–2.04 (m, 6 H), 2.02 (s, 3 H); δ_C($CDCl_3$) 170.2, 170.0, 170.0, 169.2, 152.0 ($^1J_{C,F}$ = 253.2 Hz), 149.7 ($^3J_{C,F}$ = 11.0 Hz), 143.2, 120.3 ($^4J_{C,F}$ = 3.7 Hz), 118.4, 112.9 ($^2J_{C,F}$ = 23.4 Hz), 100.1, 71.6, 70.3, 68.1, 66.6, 61.2, 20.6, 20.6, 20.5; Calcd for $C_{20}H_{22}FNO_{12}$ C, 49.29; H, 4.55; N, 2.87. Found: C, 49.26; H, 4.61; N, 2.89.

2-Chloro-4-nitrophenyl-tetra-*O*-acetyl-β-D-galactopyranoside.[8,17] (4k). Off-white solid; mp 148–149 °C (lit.[17] mp 147–149 °C); R_f 0.30 (SiO_2, cyclohexane–ethyl acetate = 3/2, v/v); δ_H ($CDCl_3$) 8.30 (d, 2.5, 1 H), 8.17–8.11 (m, 1 H), 7.29–7.27 (d, 10.4 Hz, 1 H), 5.62 (dd, 10.4, 7.8, 1 H), 5.50 (dd, 3.4, 0.9, 1 H), 5.18–5.08 (m, 1 H), 4.31–4.08 (m, 2 H), 2.20 (s, 3 H), 2.10 (s, 3 H), 2.08 (s, 3 H), 2.03 (s, 3 H); δ_C ($CDCl_3$) 170.3, 170.1, 170.1, 169.2, 157.3, 143.1, 126.2, 125.4, 124.8, 124.5, 123.5, 116.3, 116.2, 99.9, 71.6, 70.3, 67.8, 66.6, 61.3, 20.7, 20.6, 20.6, 20.5.; Calcd for $C_{20}H_{22}ClNO_{12}$: C, 47.68; H, 4.40. Found: C, 47.81; H, 4.30.

4-Chloro-3-nitrophenyl-tetra-*O*-acetyl-β-D-galactopyranoside (4m). Off-white solid; mp 121–122 °C; R_f 0.36 (SiO_2, cyclohexane–ethyl acetate = 3/2); δ_H ($CDCl_3$) 7.57 (d, 3.0, 1 H), 7.47 (d, 8.8, 1 H), 7.17 (dd, 9.0, 2.9, 1 H), 5.55–5.44 (m, 2 H), 5.13 (dd, 10.5, 3.4, 1 H), 5.09 (d, 7.8, 1 H), 4.18 (dd, 6.2, 1.6, 2 H), 4.13 (dd, 6.3, 1.0, 1 H), 2.19 (s, 3 H), 2.09 (d, 0.5, 6 H), 2.02 (s, 3 H); δ_C ($CDCl_3$) 170.5, 170.1, 170.0, 169.2, 155.2, 148.0, 132.6, 122.4, 121.1, 113.5, 99.2, 71.7, 70.5, 68.2, 66.8, 61.7, 20.7, 20.6, 20.5, 20.5; Calcd for $C_{20}H_{22}ClNO_{12}$ C, 47.68; H, 4.40; N, 2.78. Found: C, 47.79; H, 4.51; N, 2.77.

3-Nitrophenyl-tetra-*O*-acetyl-β-D-galactopyranoside (4n). Off-white solid; mp 103–104 °C, R_f 0.27 (SiO_2, cyclohexane–ethyl acetate = 2/1, v/v); δ_H ($CDCl_3$) 7.97 (dt, 8.2, 1.0, 1 H), 7.90 (t, 2.3, 1 H), 7.48 (t, 8.2, 1 H), 7.35–7.32 (m, 1 H), 5.53 (dd, 10.4, 7.9, 1 H), 5.50 (d, 3.5, 1 H), 5.16–5.13 (m, 2 H), 4.22–4.14 (m, 3 H), 2.20 (s, 3 H), 2.11 (s, 3 H), 2.10 (s, 3 H), 2.03 (s, 3 H) δ_C ($CDCl_3$) 170.6, 170.1, 170.0, 169.3, 157.0, 149.1, 130.2, 123.7, 118.2, 111.3, 99.2, 71.7, 70.6, 68.3, 66.9, 61.8, 20.7, 20.6, 20.6, 20.6; Anal. Calcd for $C_{20}H_{23}NO_{12}$ C, 51.18; H, 4.94; N, 2.98. Found: C, 51.46; H, 5.03; N, 3.05.

3-Methyl-2-nitrophenyl-tetra-*O*-acetyl-β-D-galactopyranoside (4o). Off-white solid; mp 167–168 °C; R_f 0.32 (SiO_2, cyclohexane–ethyl acetate = 3/2, v/v); δ_H ($CDCl_3$) 7.30 (t, 7.8, 1H), 7.15 (d, 8.3, 1H), 7.02 (d, 7.8, 1H), 5.42–5.53 (m, 2H), 5.08 (dd, 10.5, 3.5, 1H), 4.98 (d, 8.0, 1H), 4.27 (dd, 11.5, 7.0, 1H), 4.17 (dd, 11.0, 6.3, 1H), 4.06 (t, 6.3, 1H), 2.31 (s, 3H), 2.19 (s, 3H), 2.14 (s, 3H), 2.08 (s, 3H), 2.01 (s, 3H); δ_C ($CDCl_3$) 170.3, 170.2, 170.1, 169.3, 147.8, 143.3, 131.1, 130.5, 125.8, 115.9, 100.9, 71.3, 70.5, 67.7, 66.7, 61.3, 20.6, 20.5, 20.5, 16.9; Calcd for $C_{21}H_{25}NO_{12}$ C, 52.17; H, 5.21; N, 2.90. Found: C, 52.35; H, 5.30; N, 2.89.

4-Methoxy-2-nitrophenyl-tetra-*O*-acetyl-β-D-galactopyranoside (4p). Off-white solid; mp 157–158 °C; R_f 0.29 (SiO_2, cyclohexane–ethyl acetate = 3/2, v/v); δ_H ($CDCl_3$) 7.33 (d, 9.3 Hz, 1 H), 7.04 (dd, 9.1, 3.3, 1 H), 5.50 (dd, 10.5, 8.8, 1 H), 5.45 (dd, 3.3, 1.0, 1 H), 5.09 (dd, 10.5, 3.4, 1 H), 4.96 (d, 8.1, 1 H), 4.25 (dd, 11.2, 6.9, 1 H), 4.15 (dd, 11.2, 6.4, 1 H), 4.04–3.96 (m, 1 H), 3.83 (s, 2 H), 2.19 (s, 3 H), 2.14 (s, 3 H), 2.05 (s, 3 H), 2.01 (s, 3 H); δ_c ($CDCl_3$) 170.3, 170.2, 170.1, 169.6, 155.6, 142.8, 123.0, 119.9, 109.1, 101.6, 71.2, 70.5, 67.9, 66.7, 61.2, 56.0, 20.7, 20.6, 20.5; Calcd for $C_{21}H_{25}NO_{13}$ C, 50.50; H, 5.05; N, 2.80. Found: C, 50.60; H, 5.14; N, 2.78.

2-Methyl-4-nitrophenyl-tetra-*O*-acetyl-β-D-galactopyranoside (4q). Colorless solid; mp 128–129 °C, R_f 0.52 (SiO_2, cyclohexane–ethyl acetate = 1/1, v/v); δ_H ($CDCl_3$) 8.07–8.05 (m, 2 H), 7.07–7.04 (m, 1 H), 5.59 (dd, 10.5, 7.8, 1 H), 5.50 (d, 3.3, 1 H), 5.15 (dd, 12.0, 4.0, 1 H), 5.13 (d, 8.0, 1 H), 4.26–4.13 (m, 3 H), 2.25 (s, 3 H), 2.20 (s, 3 H), 2.08 (s, 6 H), 2.03 (s, 3 H); δ_C ($CDCl_3$) 170.3, 170.1, 170.0, 169.2, 159.5, 142.7, 129.0, 126.4, 123.1, 113.5, 98.8, 71.4, 70.5, 68.2, 66.7, 61.3, 20.7, 20.6, 20.6, 20.5, 16.2; Calcd for $C_{21}H_{25}NO_{12}$ C, 52.17; H, 5.21. Found: C, 52.18; H, 5.18.

3-Methyl-4-nitrophenyl-tetra-*O*-acetyl-β-D-galactopyranoside (4r). Off-white solid; mp 100–101 °C; R_f 0.28 (SiO_2, cyclohexane–ethyl acetate = 3/2, v/v); δ_H ($CDCl_3$) 8.21–7.86 (m, 1 H), 7.06–6.77 (m, 1 H), 5.57–5.43 (m, 1 H), 5.22–5.02 (m, 1 H), 4.32–4.05 (m, 2 H), 2.63 (s, 3 H), 2.20 (s, 3 H), 2.08 (s, 3 H), 2.03 (s, 3 H); δ_C ($CDCl_3$) 170.3, 170.1, 170.0, 169.3, 159.6, 144.0, 136.9, 127.2, 120.1, 114.1, 100.0, 98.5, 71.4, 70.6, 68.3, 66.7, 61.4, 21.4, 20.7, 20.6, 20.6, 20.5; Calcd for $C_{21}H_{25}NO_{12}$ C, 52.17; H, 5.21; N, 2.90. Found: C, 52.10; H, 5.22; N, 2.91.

General procedure yielding aryl-β-D-galactopyranosides. The title compounds were obtained by deacetylation of 3–4 g (6–8 mmol) aryl-tetra-*O*-acetyl-β-D-galactopyranosides **4a–r** in 50 mL of 7 N ammonia in methanol. The peracetylated glycosides were dissolved in the reagent, stirred at ambient temperature over 24 h. The title compounds were subsequently isolated by filtration from the suspensions in very good to excellent yields (90–95%).[8]

4-Methyl-2-nitrophenyl-β-D-galactopyranoside (2b). Off-white solid; mp 197–199 °C; R_f 0.36 (SiO_2, ethyl acetate–methanol = 9/1, v/v); δ_H (DMSO-d_6) 7.65 (d, 1.5, 1H), 7.43 (ddd, 8.5, 2.3, 0.5, 1H), 7.30 (d, 8.5, 1H), 5.11 (d, 5.3, 1H), 4.97 (d, 7.8, 1H), 4.87 (d, 6.0, 1H), 4.64 (t, 5.5, 1H), 4.56 (d, 4.5, 1H), 3.69 (t, 3.9, 1H), 3.43–3.63 (m, 4H), 3.39 (ddd, 9.3, 6.0, 3.3, 1H), 2.31 (s, 3H); δ_C (DMSO-d_6) 147.5, 140.0, 134.5, 131.3, 124.5, 117.0, 101.2, 75.7, 73.4, 70.0, 68.0, 60.2, 19.6; Calcd for $C_{13}H_{17}NO_8$ C, 49.52; H, 5.43; N, 4.44; found: C, 49.48; H, 5.51; N, 4.39.

4-Fluoro-2-nitrophenyl-β-D-galactopyranoside (2c). Off-white solid; mp 179–181 °C; R_f 0.36 (SiO_2, ethyl acetate–methanol = 9/1, v/v); δ_H (DMSO-d_6) 7.86 (dd, 8.0, 2.7, 1 H), 7.67–7.50 (m, 1 H), 7.50–7.32 (m, 1 H), 5.18 (d, 5.1, 1 H), 4.99 (d, 7.6, 1 H), 4.91 (d, 5.8, 1 H), 4.77–4.52 (m, 2 H), 3.69 (br. s., 1 H), 3.66–3.59 (m, 1 H), 3.59–3.44 (m, 3 H), 3.44–3.30 (m, 2 H); δ_C (DMSO-d_6) 155.3 ($^1J_{C,F}$ = 241.0 Hz), 146.1 ($^4J_{C,F}$ = 2.2 Hz), 140.1 ($^3J_{C,F}$ = 8.8 Hz), 120.8 ($^2J_{C,F}$ = 23.4 Hz), 118.9 ($^3J_{C,F}$ = 8.1 Hz), 111.8 ($^2J_{C,F}$ = 27.8 Hz), 101.6, 75.8, 73.3, 70.0, 68.0, 60.3; Calcd for $C_{12}H_{14}FNO_8$ C, 45.15; H, 4.42; N, 4.39. Found: C, 44.89; H, 4.47; N, 4.32.

4-Chloro-2-nitrophenyl-β-D-galactopyranoside (2d). Off-white solid; mp 207–208 °C; R_f 0.38 (SiO_2, ethyl acetate–methanol = 9/1, v/v); δ_H (DMSO-d_6) 8.02 (d, 2.5, 1 H), 7.71 (dd, 9.1, 2.5, 1 H), 7.45 (d, 9.1, 1 H), 5.20 (d, 5.3, 1 H), 5.04 (d, 7.6, 1 H), 4.92 (d, 6.1, 1 H), 4.67 (t, 5.4, 1 H), 4.62 (d, 4.3, 1 H), 3.72–3.61 (m, 2 H), 3.59–3.36 (m, 4 H); δ_C (DMSO-d_6) 148.4, 140.5, 133.6, 125.0, 124.2, 118.8, 101.1, 75.8, 73.3, 69.9, 67.9, 60.2; Calcd for $C_{12}H_{14}ClNO_8$ C, 42.93; H, 4.20; N, 4.17. Found: C, 43.01; H, 4.07; N, 4.03.

4-Bromo-2-nitrophenyl-β-D-galactopyranoside (2e). Off-white solid; mp 207–208 °C; R_f 0.36 (SiO_2, ethyl acetate–methanol = 9/1, v/v); δ_H (DMSO-d_6) 8.12 (d, 2.5, 1H), 7.83 (dd, 9.0, 2.5, 1H), 7.39 (d, 9.3, 1H), 5.20 (d, 5.3, 1H), 5.05 (d, 7.8, 1H), 4.92 (d, 6.0, 1H), 4.67 (t, 5.5, 1H), 4.62 (d, 4.5, 1H), 3.70 (t, 3.9, 1H), 3.64 (t, 6.0, 1H), 3.45–3.60 (m, 3H), 3.40 (ddd, 9.3, 6.0, 3.3, 1H); δ_C (DMSO-d_6) 148.7, 140.8, 136.4, 126.9, 119.1, 112.3, 101.1, 75.8, 73.3, 69.9, 67.9, 60.2; Calcd for $C_{12}H_{14}BrNO_8$ C, 37.91; H, 3.71; N, 3.68. Found: C, 37.93; H, 3.77; N, 3.65.

5-Fluoro-2-nitrophenyl-β-D-galactopyranoside.[8] (2f). Off-white solid; mp 173–174 °C; R_f 0.45 (SiO_2, ethyl acetate–methanol = 9/1, v/v); δ_H (DMSO-d_6) 8.00 (dd, 9.1, 6.1, 1 H), 7.32 (dd, 11.1, 2.5, 1 H), 7.04 (ddd, 8.8, 7.8, 2.5, 1 H), 5.23 (d, 5.3, 1 H), 5.10 (d, 7.6, 1 H), 4.94 (d, 6.1, 1 H), 4.70 (t, 5.6, 1 H), 4.63 (d, 4.5, 1 H), 3.70 (t, 3.8, 2 H), 3.64–3.45 (m, 3 H), 3.40 (ddd, 9.4, 6.0, 3.3, 1 H); δ_C (DMSO-d_6) 164.5 ($^1J_{C,F}$ = 251.8 Hz), 151.8 ($^3J_{C,F}$ = 12.4 Hz), 136.6, 127.4 ($^3J_{C,F}$ = 11.7 Hz), 108.7 ($^2J_{C,F}$ = 24.2 Hz), 104.7 ($^2J_{C,F}$ = 27.8 Hz), 101.0, 75.9, 73.3, 69.9, 68.0, 60.3; Anal. Calcd for $C_{12}H_{14}FNO_8$: C, 45.15; H, 4.42. Found: C, 45.18; H, 4.80.

5-Methyl-2-nitrophenyl-β-D-galactopyranoside (2g). Off-white solid; mp 150–151 °C; R_f 0.39 (SiO_2, ethyl acetate–methanol = 9/1, v/v); δ_H (DMSO-d_6) 7.75 (d, 8.3, 1H), 7.24 (s, 1H), 6.97 (dt, 8.3, 1.0, 1H), 5.14 (d, 5.3, 1H), 5.02 (d, 7.8, 1H), 4.90 (d, 6.3, 1H), 4.68 (t, 5.5, 1H), 4.60 (d, 4.5, 1H), 3.70 (t, 4.0, 1H), 3.63 (t, 6.0, 1H), 3.50–3.60 (m, 2H), 3.47 (dd, 10.8, 5.8, 1H), 3.36–3.43 (m, 1H), 2.37 (s, 3H); δ_C (DMSO-d_6) 149.9, 145.2, 137.8, 124.7, 122.1, 117.3, 101.0, 75.7, 73.4, 70.1, 68.0, 60.2, 21.4; Calcd for $C_{13}H_{17}NO_8$ C, 49.52; H, 5.43; N, 4.44. Found: C, 49.28; H, 5.40; N, 4.43.

2-Fluoro-4-nitrophenyl-β-D-galactopyranoside.[8] (2i). Off-white solid; mp 188–189 °C; R_f 0.39 (SiO_2, ethyl acetate–metha-

nol = 9/1, v/v); δ_H (DMSO-d_6 8.20 (dd, 10.8, 2.8, 1H), 8.10 (ddd, 9.2, 2.7, 1.4, 1H), 7.49 (t, 9.0, 1H), 5.36 (d, 5.5, 1H), 5.15 (d, 7.8, 1H), 4.97 (d, 5.8, 1H), 4.68 (t, 5.5, 1H), 4.62 (d, 4.8, 1H), 3.72 (t, 4.0, 1H), 3.61–3.70 (m, 2H), 3.55 (dd, 11.0, 5.8, 1H), 3.47–3.52 (m, 1H), 3.41–3.47 (m, 1H); δ_C (DMSO-d_6) 150.8 ($^2J_{C,F}$ = 10.2 Hz), 150.5 ($^1J_{C,F}$ = 249.6 Hz), 141.0 ($^3J_{C,F}$ = 7.3 Hz), 121.1 ($^3J_{C,F}$ = 2.9 Hz), 116.5, 112.4 ($^2J_{C,F}$ = 23.4 Hz), 100.7, 75.9, 73.2, 69.9, 68.0, 60.2; Calcd for $C_{12}H_{14}FNO_8$ C, 45.15; H, 4.42; N, 4.39. Found: C, 44.89; H, 4.56; N, 4.35.

2-Chloro-4-nitrophenyl-β-D-galactopyranoside.[8,17] (2k). Off-white solid; mp 210–211 °C (lit.[5] mp 213–215 °C); R_f 0.33 (SiO_2, ethyl acetate–methanol = 9/1, v/v); δ_H (DMSO-d_6) 8.33 (d, 2.8, 1 H), 8.20 (dd, 9.3, 2.8, 1 H), 7.46 (d, 9.3, 1 H), 5.29 (d, 5.6, 1 H), 5.18 (d, 7.8, 1 H), 4.97 (d, 5.8, 1 H), 4.74–4.59 (m, 2 H), 3.77–3.61 (m, 3 H), 3.59–3.39 (m, 3 H); δ_C (DMSO-d_6) 157.9, 141.4, 125.5, 124.2, 122.2, 115.6, 100.6, 75.9, 73.3, 69.9, 68.0, 60.2; Calcd for $C_{12}H_{14}ClNO_8$ C, 42.93; H, 4.20; N, 4.17. Found: C, 42.87; H, 4.16; N, 4.13.

4-Chloro-3-nitrophenyl-β-D-galactopyranoside (2m). Off-white solid, mp 176–178 °C, R_f 0.50 (SiO_2, ethyl acetate–methanol = 5/1, v/v); δ_H (DMSO-d_6) 7.10 (d, 2.8, 1 H), 7.69 (d, 9.2, 1 H), 7.36 (dd, 8.8, 2.8, 1 H), 5.27 (d, 5.2, 1 H), 4.95 (d, 8.0, 1 H), 4.93 (d, 5.6, 1 H), 4.67 (t, 5.6, 1 H), 4.57 (d, 4.4, 1 H), 3.70 (t, 4.0, 1 H), 3.63 (t, 6.4, 1 H), 3.60–3.45 (m, 3 H), 3.43–3.38 (m, 1 H); δ_C (DMSO-d_6) 156.4, 148.1, 132.2, 121.9, 116.9, 113.1, 101.1, 75.7, 73.1, 70.0, 68.0, 60.2; HRMS (ESI): m/z Calcd for $C_{12}H_{14}ClNO_8$ $[M + Na]^+$: 358.0306; Found: 358.0291.

3-Nitrophenyl-β-D-galactopyranoside (2n). Off-white solid after chromatographic purification on silica gel (ethyl acetate–CH_2Cl_2–methanol = 10/10/5); mp 175–177 °C, R_f 0.33 (SiO_2, ethyl acetate–methanol, 10/1, v/v); δ_H (DMSO-d_6) 7.87 (dd, 7.8, 1.8, 1H), 7.82 (t, 2.3, 1H), 7.60 (t, 8.3, 1H), 7.49 (dd, 8.0, 1.8, 1H), 5.27 (d, 5.0, 1H), 4.97 (d, 7.8, 1H), 4.93 (d, 5.5, 1H), 4.69 (t, 5.5, 1H), 4.57 (d, 4.8, 1H), 3.71 (t, 3.8, 1H), 3.63–3.68 (m, 1H), 3.61 (dt, 7.5, 2.0, 1H), 3.56 (dd, 11.0, 6.0, 1H), 3.50 (dd, 12.3, 5.3, 1H), 3.44 (ddd, 9.3, 5.8, 3.4, 1H); δ_C (DMSO-d_6) 157.9, 148.6, 130.7, 123.3, 116.7, 110.9, 101.2, 75.7, 73.1, 70.2, 68.1, 60.3; Calcd for $C_{12}H_{15}NO_8$ C, 47.84; H, 5.02; N, 4.65. Found: C, 47.68; H, 5.06; N, 4.57.

3-Methyl-2-nitrophenyl-β-D-galactopyranoside (2o). Off-white solid after chromatographic purification over silica gel using ethyl acetate–CH_2Cl_2–MeOH = 10/10/4, v/v/v) as eluent; mp 149–154 °C; R_f 0.52 (SiO_2, ethyl acetate–methanol = 5/1, v/v); δ_H (DMSO-d_6) 7.41 (t, 7.7, 1H), 7.22 (d, 8.5, 1H), 7.04 (dd, 7.7, 0.6, 1H), 5.11 (d, 5.5, 1H), 4.98 (d, 7.8, 1H), 4.88 (d, 1.0, 1H), 4.66 (t, 5.5, 1H), 4.58 (d, 4.5, 1H), 3.68 (t, 3.6, 1H), 3.61 (t, 6.3, 1H), 3.54 (dd, 11.3, 6.0, 1H), 3.43–3.51 (m, 2H), 3.35–3.42 (m, 1H), 2.23 (s, 3H); δ_C (DMSO-d_6) 148.2, 141.8, 131.0, 130.0, 123.6, 113.9, 101.0, 75.8, 73.4, 70.0, 68.0, 60.3, 16.3; HRMS (ESI): m/z Calcd for $C_{13}H_{17}NO_8$ $[M + Na]^+$: 338.0852; Found: 338.0845.

4-Methoxy-2-nitrophenyl-β-D-galactopyranoside (2p). Off-white solid; mp 199–200 °C; R_f = 0.52 (SiO_2, ethyl acetate–methanol = 5/1, v/v); δ_H (DMSO-d_6) 7.41 (d, 3.0, 1 H), 7.36 (d, 9.3, 1 H), 7.22 (dd, 9.3, 3.0, 1 H), 5.11 (d, 5.3, 1 H), 4.89 (d, 1.5, 1 H), 4.87 (s, 1 H), 4.67–4.61 (m, 1 H), 4.57 (d, 4.3, 1 H), 3.78 (s, 3 H), 3.68 (t, 3.9, 1 H), 3.60–3.35 (m, 5H); δ_C (DMSO-d_6) 153.4, 143.4, 140.7, 120.0, 118.9, 108.9, 102.0, 75.7, 73.3, 70.1, 68.0, 60.2, 56.0; Calcd for $C_{13}H_{17}NO_9$ C, 47.13; H, 5.17; N, 4.23. Found: C, 46.97; H, 5.12; N, 4.19.

2-Methyl-4-nitrophenyl-β-D-galactopyranoside (2q). Colorless solid after chromatographic purification on silica gel (ethyl acetate–CH_2Cl_2–MeOH = 5/5/2, v/v/v); mp 245–246 °C, R_f 0.22 (SiO_2, ethyl acetate–methanol = 9/1, v/v); δ_H (DMSO-d_6) 8.10–8.06 (m, 2 H), 7.24 (d, 9.0, 1 H), 5.29 (dd, 5.1, 0.6, 1 H), 5.00 (d, 7.5, 1 H), 4.94 (d, 5.0, 1 H), 4.68 (t, 5.1, 1 H), 4.59 (d, 4.5, 1 H), 3.72 (t, 3.8, 1 H), 3.68–3.63 (m, 2 H), 3.58–3.42 (m, 2 H), 2.29 (s, 3 H); δ_C (DMSO-d_6) 160.8, 141.1, 128.1, 125.7, 123.3, 113.9, 100.7, 75.7, 73.1, 70.2, 68.0, 60.3, 15.9; Calcd for $C_{13}H_{17}NO_8$ C, 49.52; H, 5.43. Found: C, 49.44; H, 5.38.

3-Methyl-4-nitrophenyl-β-D-galactopyranoside (2r). Off-white solid after chromatographic purification on silica gel (ethyl acetate–CH_2Cl_2–MeOH = 2/2/1, v/v/v); mp 184–186 °C; R_f 0.38 (SiO_2, ethyl acetate–MeOH = 9/1, v/v); δ_H (DMSO-d_6) 8.04 (d, 9.0, 1 H), 7.09 (s, 1 H), 7.05 (dd, 9.0, 2.3, 1 H), 5.25 (d, 5.3, 1 H), 4.99 (d, 7.8, 1 H), 4.92 (d, 5.8, 1 H), 4.67 (t, 5.5, 1 H), 4.56 (d, 4.5, 1 H), 3.71 (t, 3.8, 1 H), 3.66–3.61 (m, 1 H), 3.60–3.47 (m, 3 H), 3.44–3.40 (m, 1 H), 2.54 (s, 3 H); δ_C (DMSO-d_6) 160.8, 142.5, 136.1, 127.1, 119.5, 114.3, 100.5, 75.7, 73.2, 70.0, 60.3, 20.7; Calcd for $C_{13}H_{17}NO_8$: C, 49.52; H, 5.43; N, 4.44. Found: C, 49.35; H, 5.57; N, 4.29.

Kinetic assays

Molar absorptivity of the phenols. Typically, 5 mg of a phenol were dissolved in 25 mL of 50 mM acetate buffer at pH 5.0. Subsequently, 10–50 μL aliquots of the solution were diluted into 100 μL volumes in 96-well plates by addition of buffer yielding 0.1–0.7 mM phenol solutions. The solutions were thoroughly mixed and then equilibrated at 30.0 ± 0.1 °C for 30 min prior to determination of their absorbance at 405 nm. The obtained absorbance values were plotted *versus* known phenol concentrations. The linear fit of the data equals the product of extinction coefficient ε_{405} times the unknown path length d for product absorbance in 96-well plates containing 100 μL solutions in 50 mM acetate buffer at pH 5.0. For each phenol, three independent experiments were performed and the data averaged. The extinction coefficients summarized (Table 1) are corrected by the path length using the information by the manufacturer for the correlation between path length and cell filling volume.

Enzyme stock solution. Typically, 3–5 mg of β-galactosidase (*A. oryzae*) were dissolved in 5 mL of 50 mM acetate buffer at pH 5.0. Subsequent dilution of 250 μL of this solution into a 5 mL volume yielded a 3×10^{-8} M enzyme stock solution.

Substrate stock solution. Typically, 7–10 mg substrate were dissolved in 5.0 mL of 50 mM acetate buffer at pH 5.0 yielding 15–20 mM substrate stock solutions.

Inhibitor stock solution. Typically, 50 μM inhibitor solutions in nanopure water were kept frozen at −18 °C and

thawed when needed. Serial dilution in nanopure water yielded 0.25–1.0 μM inhibitor stock solutions that were used for the inhibited enzymatic substrate hydrolysis described below.

Assay for enzymatic substrate hydrolysis. The substrate stock solution was placed in 10–70 μL aliquots in 96-well plates and diluted with acetate buffer into solutions with an overall volume of 80 μL. These solutions were equilibrated at 30.0 ± 0.1 °C for 30 min. The enzymatic hydrolysis was then initiated by addition of a 20 μL aliquot of the enzyme stock solution followed by thorough mixing. The product formation was monitored at 405 nm using UV/Vis spectroscopy over the initial 15 min of the reaction. A typical final substrate concentration in the assay was 5–40 μM, the overall aliquot volume was 100 μL.

The absorbance recorded was plotted *versus* time in minutes. The rate of the reaction was determined at each substrate concentration from the slope of the linear fit of the data after conversion of the absorbance into product concentration using the calibration curves described above. The rate of the reaction was corrected for the enzyme concentration and the uncatalyzed reaction, and then plotted *versus* the substrate concentration. By applying a non-linear fit of the resulting hyperbolic data, the catalytic rate constant k_{cat} [min^{-1}] and the substrate affinity K_M [mM] were discerned utilizing the Michaelis–Menten model. All experiments were conducted in triplicate and the data were averaged.

Assay for the inhibited enzymatic substrate hydrolysis. The assay was prepared as described earlier, but 10 μL of the buffer solution were substituted by 10 μL of the inhibitor stock solution. The enzymatic catalysis was initiated and monitored as described above.

Apparent Michaelis–Menten constants (K'_m) and rate constants (k'_{cat}) were determined by plotting the initial rates corrected for the enzyme concentration *versus* the substrate concentration, and fitting the hyperbolic data by non-linear regression. Typically, kinetic parameters for three different inhibitor concentrations were determined. The inhibition constant (K_i) for competitive inhibition was calculated from eqn (1), where K'_m and K_m are Michaelis–Menten constants in the presence and absence of the inhibitor:

$$K'_m = K_m \times (1 + ([I]/K_i)) \quad (1)$$

All experiments were conducted in triplicate for each inhibitor concentration, and the data were averaged.

Stability assays

Amidine stock solution. A 0.168 M stock solution of **1d** (30.69 mg, 0.109 mmol) in 0.650 mL of nanopure water was prepared and kept at ambient temperature. Aliquots of this solution were used for all amidine stability assays described below.

Amidine stability assay. Solutions of 740 μL of nanopure water or of 50 mM acetate buffer at pH 5 were respectively thermostated in a modular heating block at 30, 50 or 72 °C for 1 h. Then, 60 μL (2.83 mg, 10.11 μmol) of the amidine stock solution described above were added respectively.

Subsequently, 60 μL aliquots of the equilibrated solutions were taken in regular time intervals at 0, 5, 10 15, 20, 25, 30, 40, 50, 60, 75, and 90 min. The aliquots were immediately submerged into liquid nitrogen and stored at −18 °C prior to HPLC analysis. The equilibrating solutions were periodically mixed thoroughly throughout the entire experiment time.

Amidine quantification assay. All experiments were conducted on a Shimadzu HPLC with a Rezex-Carbohydrate Na^+ (8%) column 300 × 7.8 mm and 50 × 7.8 mm guard column (Phenomenex) using nanopure water as eluent with a flow rate of 0.4 mL min^{-1} at 80 °C. Immediately prior to analysis, the frozen samples were thawed and subjected to analysis in 10 μL aliquots. The elution was followed for 60 min. Galactonoamidine **1d** elutes at 10.6 min.

Acknowledgements

An undergraduate research fellowship of the University of Arkansas Honors College to R.G.L. and support by the National Science Foundation (CHE-1244755, CHE-1305543) to S. S. are gratefully acknowledged. This study was furthermore supported by Grant Number P30 GM103450 from the National Institute of General Medical Sciences (NIGMS) of the National Institutes of Health (NIH).

Notes and references

1 M.-P. Heck, S. P. Vincent, B. W. Murray, F. Bellamy, C.-H. Wong and C. Mioskowski, *J. Am. Chem. Soc.*, 2004, **126**, 1971–1979.
2 P. A. Bartlett and C. K. Marlowe, *Biochemistry*, 1983, **22**, 4618–4624.
3 M. A. Phillips, A. P. Kaplan, W. J. Rutter and P. A. Bartlett, *Biochemistry*, 1992, **31**, 959–963.
4 R. C. Thompson, *Biochemistry*, 1973, **12**, 47–51.
5 T. M. Gloster and G. J. Davies, *Org. Biomol. Chem.*, 2010, **8**, 305–320.
6 R. Kanso, E. A. Yancey and S. Striegler, *Tetrahedron*, 2012, **68**, 47–52.
7 R. Kanso and S. Striegler, *Carbohydr. Res.*, 2011, **346**, 897–904.
8 L. Kröger and J. Thiem, *Carbohydr. Res.*, 2007, **342**, 467–481.
9 Y. Bleriot, T. Dintinger, A. Genre-Grandpierre, M. Padrines and C. Tellier, *Bioorg. Med. Chem. Lett.*, 1995, **5**, 2655–2660.
10 Y. Bleriot, A. Genre-Grandpierre and C. Tellier, *Tetrahedron Lett.*, 1994, **35**, 1867–1870.
11 B. Ganem, *Acc. Chem. Res.*, 1996, **29**, 340–347.
12 B. Ganem and G. Papandreou, *J. Am. Chem. Soc.*, 1991, **113**, 8984–8985.
13 Y. T. Pan, G. P. Kaushal, G. Papandreou, B. Ganem and A. D. Elbein, *J. Biol. Chem.*, 1992, **267**, 8313–8318.

14 M. K. Tong, G. Papandreou and B. Ganem, *J. Am. Chem. Soc.*, 1990, **112**, 6137–6139.
15 M. Hunsen, D. A. Long, C. R. D'Ardenne and A. L. Smith, *Carbohydr. Res.*, 2005, **340**, 2670–2674.
16 A. I. Vogel, B. S. Furniss, A. J. Hannaford, P. W. G. Smith and A. R. Tatchell, *Vogel's textbook of practical organic chemistry*, Longman, Edinburgh, 1989.
17 D. R. Hwang and M. E. Scott, *Bioorg. Chem.*, 1993, **21**, 284–293.